Intelligent Volt Var Control in Active Distribution Networks

SID: 510075642

May 2025

Contents

1 Part 1: Day-Ahead Dispatch with Conventional VVC **2**
1.1 Background . . . 3
1.2 Case Studies . . . 3
1.2.1 System model . . . 4
1.2.2 Parameters of Voltage Regulation Devices . . . 4
1.3 Mathematical Formulation . . . 5
1.4 Results . . . 6
1.4.1 Case 1 and 2: OLTCs and CBs . . . 6
1.4.2 Case 3: OLTCs, CBs and PVs . . . 8

2 Part 2: Enhanced Volt/Var Control **9**
2.1 Literature Review of Enhanced VVC . . . 9
2.2 Limitation of OLTC and CB . . . 9
2.3 Multi-Timescale Hierarchical Control . . . 10
2.3.1 System model . . . 10
2.3.2 Parameters of Voltage Regulation Devices . . . 11
2.3.3 Mathematical Formulation . . . 11
2.3.4 Results . . . 13

3 MATLAB code **14**

4 Video comments **14**

Nomenclature

Sets and Indices

$t \in T$	Time periods, $T = \{1, 2, \ldots, 24\}$
$i, j \in N$	Buses in the distribution network
$ij \in E$	Lines in the distribution network connecting buses i and j
N_{CB}	Set of buses with capacitor banks
N_{PV}	Set of buses with PV generation
N_{SVC}	Set of buses with static VAR compensators
Ω_i^+	Set of incoming lines to bus i
Ω_i^-	Set of outgoing lines from bus i
K	Set of capacitor units
T^{fast}	Fast control time periods (30 seconds)
T^{coord}	Coordination control time periods (5 minutes)
T^{slow}	Slow control time periods (1 hour)

Parameters

r_{ij}, x_{ij}	Resistance and reactance of line ij [p.u.]
$P_{l,i,t}, Q_{l,i,t}$	Active and reactive power demand at bus i and time t [p.u.]
$PV_{i,t}$	Maximum available PV generation at bus i and time t [p.u.]
V_{min}, V_{max}	Minimum and maximum voltage magnitude limits [p.u.]
V_s	Substation base voltage [p.u.]
V_{nom}	Nominal voltage magnitude [p.u.]
$V_{ref,i}$	Voltage reference setpoint at bus i [p.u.]
V_{target}	Target voltage for coordination layer [p.u.]
ΔV_T	Voltage step size of OLTC transformer [p.u.]
tap_{max}	Maximum tap changer position
$cap_{ik,max}$	Maximum number of switching operations for capacitor bank
q_{ik}	Reactive power provided by one capacitor unit [p.u.]
$S_{PV,i,t}$	Apparent power rating of PV inverter at bus i and time t [p.u.]
$S_{rating,i}$	Apparent power rating of PV inverter at bus i [p.u.]
$Q_{SVC,max}$	Maximum SVC reactive power capability [p.u.]
K^{PV}	Global droop coefficient for PV inverters [p.u./p.u.]
K^{SVC}	Global droop coefficient for SVCs [p.u./p.u.]
α_{PV}	Coordination gain for PV setpoint adjustment [p.u./p.u.]
α_{SVC}	Coordination gain for SVC setpoint adjustment [p.u./p.u.]
Δt^{fast}	Fast control time step (30 seconds)
Δt^{coord}	Coordination control time step (5 minutes)
Δt^{slow}	Slow control time step (1 hour)

Decision Variables

$P_{ij,t}, Q_{ij,t}$	Active and reactive power flow through line ij at time t [p.u.]
$l_{ij,t}$	Square of current magnitude in line ij at time t [p.u.]
$v_{i,t}$	Square of voltage magnitude at bus i and time t [p.u.]
$P_{PV,i,t}$	Active power output from PV at bus i and time t [p.u.]
$Q_{PV,i,t}$	Reactive power output from PV at bus i and time t [p.u.]
$Q^{fast}_{PV,i,t}$	Fast-responding reactive power from PV at bus i [p.u.]
$Q^{set}_{PV,i}$	Reactive power setpoint for PV from coordination layer [p.u.]
$Q_{CB,i,t}$	Reactive power from capacitor bank at bus i and time t [p.u.]
$Q_{SVC,i,t}$	Reactive power from SVC at bus i and time t [p.u.]
$Q^{fast}_{SVC,i,t}$	Fast-responding reactive power from SVC at bus i [p.u.]
$Q^{set}_{SVC,i}$	Reactive power setpoint for SVC from coordination layer [p.u.]
tap_t	Tap position of OLTC at time t
d^t_k	Binary variable for tap position selection (= 1 if tap position k is selected)
$c_{ik,t}$	Binary variable for capacitor bank status (= 1 if bank is on)
$a_{ik,t}, b_{ik,t}$	Binary variables for modeling capacitor switching operations

1 Part 1: Day-Ahead Dispatch with Conventional VVC

In recent years, distributed generation (DG) and renewable energy sources (RES) have been increasingly integrated into distribution networks. Traditional voltage control relies on on-load tap changers (OLTC) and capacitor banks (CB), but the intermittent nature of renewables like solar PV creates new challenges, including rapid power fluctuations and voltage violations. This project focuses on developing effective, fast-responding VVC methods to address voltage violations across different operational timescales in active distribution networks.

1.1 Background

Volt-Var Control (VVC) is a coordinated control technique that manages both voltage levels and reactive power flow throughout the distribution system by optimizing various control devices including OLTCs, CBs, voltage regulators, and inverters connected to DG units. Unlike traditional voltage control methods that operate independently and reactively, VVC employs a systematic approach to maintain voltage within acceptable ranges (typically $\pm 5\%$) while minimizing power losses and improving efficiency.

The need for advanced VVC has become critical. Firstly, the bidirectional power flows created by high DG penetration can cause voltage rise issues, leading to equipment damage and system instability. Secondly, traditional control devices like OLTC and CBs have limited response speeds and discrete control steps, making them inadequate for managing rapid voltage fluctuations.

The economic implications are also important, since voltage violations can result in equipment damage, reduced equipment lifespan, and potential utility penalties for failing to maintain quality standards. Furthermore, the multi-timescale nature of VVC operation — from real-time (seconds) to day-ahead planning (hours) — requires sophisticated optimization approaches that can balance immediate operational needs with longer-term system planning objectives.

1.2 Case Studies

To comprehensively evaluate the performance of the proposed MISOCP optimization framework for distribution network control, three distinct case studies of different control variables are conducted, to analyze their impact on network operation, voltage regulation, and overall system efficiency.

- Case 1: OLTC and CBs - small load: 0.2-0.5 p.u.

  The first case establishes a baseline scenario representing conventional distribution networks with voltage control devices, under a small loading condition of 0.2-0.5 per unit. The voltage control devices include:

  - On-Load Tap Changer (OLTC) at the substation
  - Switched Capacitor Banks (CBs) at selected buses

  This configuration represents the current state of many distribution networks worldwide, where voltage regulation relies primarily on discrete control actions. The OLTC provides voltage adjustment at the substation level, while CBs offer localized reactive power compensation. This case serves as a reference point for evaluating the benefits of modern grid technologies.

- Case 2: OLTC and CBs - medium load: 0.5-1.0 p.u.

  In the second case, we increase the system demand to medium load levels of 0.5-1.0 per unit to examine how these same control devices respond to higher demand.

  This configuration evaluates how traditional voltage control devices perform under moderate stress which is common in modern distribution networks, as voltage regulation margins become tighter and reactive power requirements increase significantly.

- Case 3: Integration of PV-based DG - medium load: 0.5-1.0 p.u.

  The third case extends case 1 and 2 by incorporating photovoltaic (PV)-based distributed generation (DG) on top of the existing OLTCs and CBs, reflecting the ongoing transition toward renewable energy integration in distribution networks. This configuration adds:

  - Distributed PV systems with controllable active power output
  - PV reactive power capability within inverter limits

  The inclusion of PV generation introduces both challenges and opportunities for voltage control. While variable PV output can cause voltage fluctuations, modern inverters' reactive power capability provides additional voltage support. This case evaluates how the optimization framework adapts traditional control devices (OLTC and CBs) to accommodate renewable generation while maintaining voltage quality.

1.2.1 System model

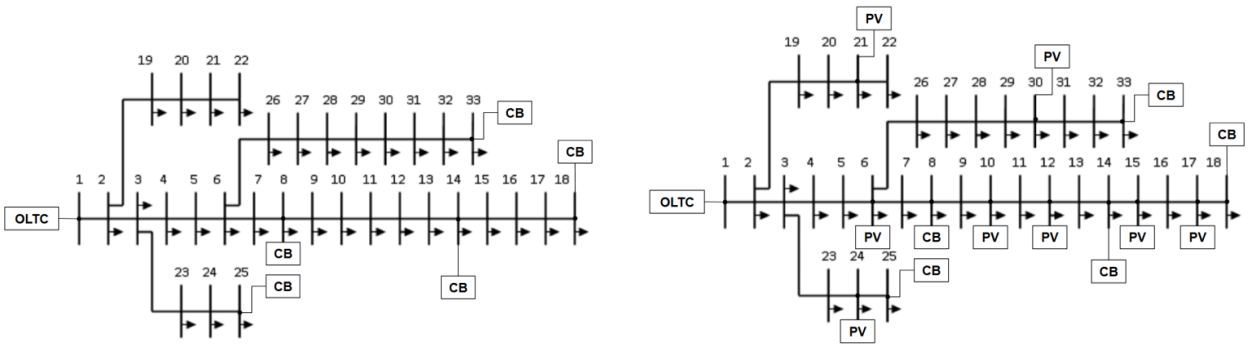

(a) case 1 and 2 (b) case 3

Figure 1: IEEE 33-bus system model of (a) OLTCs and CBs; (b) OLTCs, CBs and PVs

1. **System model: OLTCs and CBs**

   Fig.1(a) shows the base system for case 1 and 2, incorporating two conventional voltage control technologies: an On-Load Tap Changer (OLTC) with ±12.5% regulation range and 10 tap positions, and five Capacitor Banks (CBs) rated at 900 kVA each with a maximum of 6 switching operations per day located at buses 8, 14, 18, 25, and 33. The OLTC provides continuous voltage regulation, and the CBs supply reactive power compensation throughout the 24-hour operational period.

2. **System model: OLTCs, CBs and PVs**

   Fig.1(b) extends the base system, on top of the OLTC and CBs, the system adds Photovoltaic (PV) generation units totaling 600 kVA (≈46% penetration) distributed across buses 6, 10, 12, 15, 17, 21, 24, and 30. We evaluates the system under medium load conditions (0.5-1.0 p.u.). The PVs can provide local reactive power support through their inverters and reduce voltage drops by injecting power closer to loads, reducing transmission losses. However, they can also create voltage fluctuations and possible voltage rise issues due to high PV generation during low-load periods.

1.2.2 Parameters of Voltage Regulation Devices

Table 1: Parameters Of Voltage Regulation Devices

Device	Parameters	Operation Limits	Placement
OLTC	$\pm 12.5 \times 1\%$	10	1
CB1-5	900 kVar	6	8, 14, 18, 25, 33
PV1-8	600 kVA	-	6, 10, 12, 15, 17, 21, 24, 30

The proposed MISOCP-based VVC approach is evaluated on a modified IEEE 33-bus distribution network with OLTC and CBs, with the addition of PVs in case 3. The network parameters follow the standard IEEE 33-bus test system with capacity, operation parameters, and placement of voltage regulation devices as specified in Table 1. The load profiles are derived from Australia Energy Market Operator (AEMO) demand data for May 10th, 2025, while PV generation profiles are synthetically generated using realistic solar irradiance patterns with bell-curve characteristics during daylight hours (6 AM to 6 PM). The system is tested using May 10th, 2025 data with hourly resolution over a 24-hour period. The day-ahead optimization framework coordinates all voltage control devices to minimize power losses while maintaining voltage limits and device operational constraints.

Note that the voltage bound is set to 0.95 to 1.05 p.u., meaning there is a ±5% voltage variation. However in case 2, the voltage drops are too large for the OLTC range to compensate with the medium load (0.5-1.0

p.u.), and the base system cannot maintain voltage within [0.95, 1.05] p.u. bounds. So in case 2, the voltage bound is relaxed to [0.85, 1.15] p.u. (i.e., ±15% variation).

1.3 Mathematical Formulation

The proposed design is modified from the day-ahead centralized optimization problem defined in [1], and on load tap changer (OLTC) and capacitor banks (CBs) are dispatched at a one-hour time interval. We aim to minimize the total power loss in the network.

The MISOCP formulation minimizes the total power loss (1) subject to: power balance constraints (2); line flow constraints, including voltage drop constraints (3) and the SOCP relaxation of power flow (4); voltage bounds and OLTC voltage constraints (5); OLTC tap change limits (6); CB switching limits and reactive power injection (8), and PV capability constraints (10).

Equation (7) and (9) are linearization of constraints (6) and (8) respectively. And equation (11) is a piecewise linear approximation of the circular capability curve for constraint (10).

$$\min_{\substack{tap_t, c_{ik,t}, \\ P_{ij,t}, Q_{ij,t}, l_{ij,t}, v_{i,t}, \\ P_{PV,i,t}, Q_{PV,i,t}, Q_{CB,i,t}}} \sum_{t\in T}\sum_{ij\in E} r_{ij} l_{ij,t} \tag{1}$$

$$\begin{cases} P_{PV,i,t} - P_{l,i,t} = \sum_{k\in\Omega_i^+}(P_{ji,t} + r_{ji} l_{ji,t}) - \sum_{j\in\Omega_i^-} P_{ij,t} \\ Q_{PV,i,t} + Q_{CB,i,t} - Q_{l,i,t} = \sum_{k\in\Omega_i^+}(Q_{ji,t} + x_{ji} l_{ji,t}) - \sum_{j\in\Omega_i^-} Q_{ij,t} \end{cases} \quad \forall i \in N, t \in T \tag{2}$$

$$v_{j,t} = v_{i,t} - 2(r_{ij}P_{ij,t} + x_{ij}Q_{ij,t}) + (r_{ij}^2 + x_{ij}^2) l_{ij,t} \quad \forall ij \in E, t \in T \tag{3}$$

$$\left\| \begin{pmatrix} 2P_{ij,t} \\ 2Q_{ij,t} \\ l_{ij,t} - v_{i,t} \end{pmatrix} \right\|_2 \leq l_{ij,t} + v_{i,t} \quad \forall ij \in E, t \in T \tag{4}$$

$$\begin{cases} V_{min}^2 \leq v_{i,t} \leq V_{max}^2 \quad \forall i \in N, t \in T \\ v_{1,t} = (V_s + tap_t \cdot \Delta V_T)^2 \quad \forall t \in T \end{cases} \tag{5}$$

$$\sum_{t=1}^{T-1} |tap_{t+1} - tap_t| \leq tap_{max} \tag{6}$$

$$\begin{cases} tap_t = \sum_{k=-tap_{max}}^{tap_{max}} k \cdot d_k^t \\ \sum_{k=-tap_{max}}^{tap_{max}} d_k^t = 1 \\ d_k^t \in \{0,1\} \quad \forall k \in \{-tap_{max}, \ldots, tap_{max}\}, t \in T \end{cases} \tag{7}$$

$$\begin{cases} \sum_{t=1}^{T-1} |c_{ik,t+1} - c_{ik,t}| \leq cap_{ik,max} \quad \forall i \in N_{CB}, k \in K \\ Q_{CB,i,t} = \sum_k c_{ik,t} q_{ik} \quad \forall i \in N_{CB}, t \in T \end{cases} \tag{8}$$

$$\begin{cases} b_{ik,t} = c_{ik,t} + c_{ik,t+1} - 2a_{ik,t} \\ a_{ik,t} \leq c_{ik,t} \\ a_{ik,t} \leq c_{ik,t+1} \\ a_{ik,t} \geq c_{ik,t} + c_{ik,t+1} - 1 \\ c_{ik,t} \in \{0,1\} \quad \forall i \in N_{CB}, k \in K, t \in T \end{cases} \tag{9}$$

$$|Q_{PV,i,t}| \leq \sqrt{S_{PV,i,t}^2 - P_{PV,i,t}^2} \quad \forall i \in N_{PV}, t \in T \tag{10}$$

$$\begin{cases} 0 \leq P_{PV,i,t} \leq PV_{i,t} \quad \forall i \in N_{PV}, t \in T \\ Q_{PV,i,t}\cos(\theta_s) + P_{PV,i,t}\sin(\theta_s) \leq S_{PV,i,t} \quad \forall i \in N_{PV}, t \in T, s \in \{1, 2, ..., n_{segments}\} \end{cases} \tag{11}$$

1.4 Results

1.4.1 Case 1 and 2: OLTCs and CBs

The comparison between Case 1 (small load: 0.2-0.5 p.u.) and Case 2 (medium load: 0.5-1.0 p.u.) demonstrates the limitations of conventional OLTC and CB systems under increased loading. In Case 1, the voltage profiles remain relatively stable with minimal voltage deviations, requiring only some CB switching operations and infrequent OLTC tap changes (Fig.2, Fig.4). However, Case 2 shows significant voltage stress with more voltage drops and increased variability, particularly during peak load periods. This is also the reason why we relax the voltage constraints in this case from ±5% to ±15%. The OLTC also requires more frequent tap adjustments in Case 2, indicating that conventional devices are operating near their limits to maintain acceptable voltage levels. The reactive power output in Fig.3 demonstrate that CBs must operate more frequently and provide higher reactive power injection in Case 2, and the CBs are utilized more compared to selective activation in Case 1.

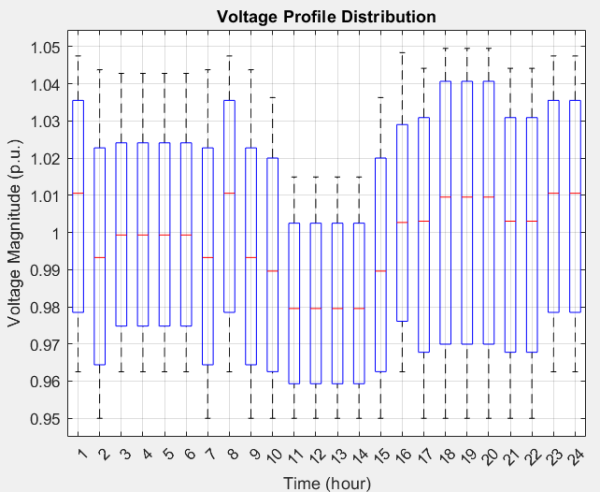

(a) case 1: 0.2-0.5 p.u.

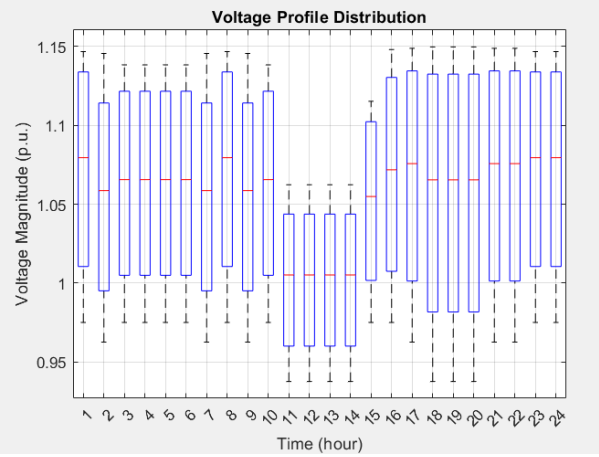

(b) case 2: 0.5-1.0 p.u.

Figure 2: Voltage profile of case 1 and 2 (OLTC+CB)

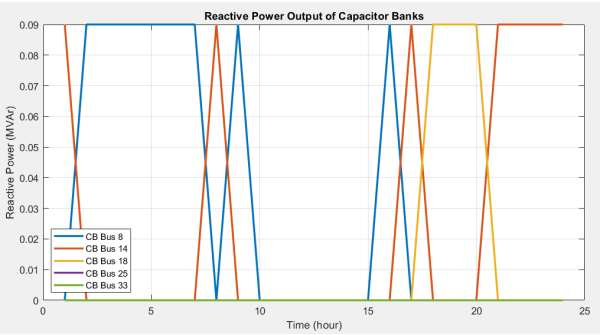

(a) case 1: 0.2-0.5 p.u.

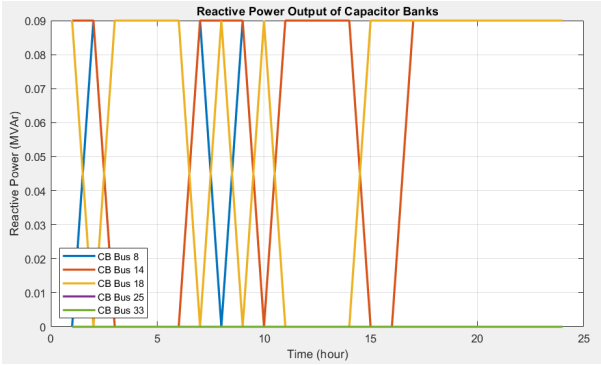

(b) case 2: 0.5-1.0 p.u.

Figure 3: Reactive power of CBs of case 1 and 2 (OLTC+CB)

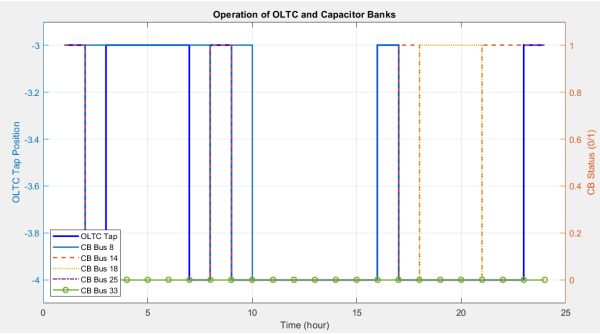

(a) case 1: 0.2-0.5 p.u.

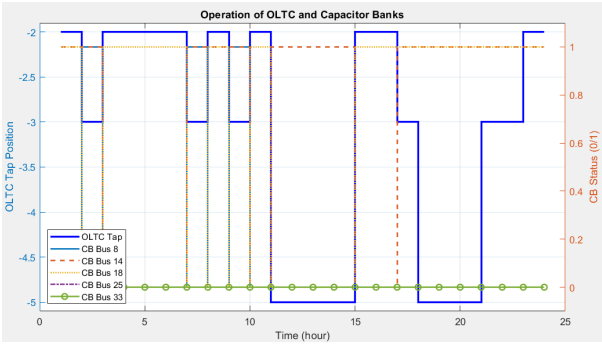

(b) case 2: 0.5-1.0 p.u.

Figure 4: Operation of OLTC and CBs of case 1 and 2 (OLTC+CB)

1.4.2 Case 3: OLTCs, CBs and PVs

The integration of PV systems in Case 3 shows substantial improvements over the conventional approach in Case 2 with the same medium load, since PVs can provide local reactive power support at their connection points, reducing the burden on centralized conventional devices and enabling more effective voltage regulation across the network. In Fig.5, the voltage profile shows better regulation with reduced voltage deviations and improved stability throughout the 24-hour period. Moreover, Fig.6 shows that the reactive power requirements from CBs are dramatically reduced, with fewer switching operations and lower reactive power injection compared to Case 2. The OLTC operation is also simplified, requiring fewer tap changes due to the distributed voltage support provided by PV inverters (Fig.7).

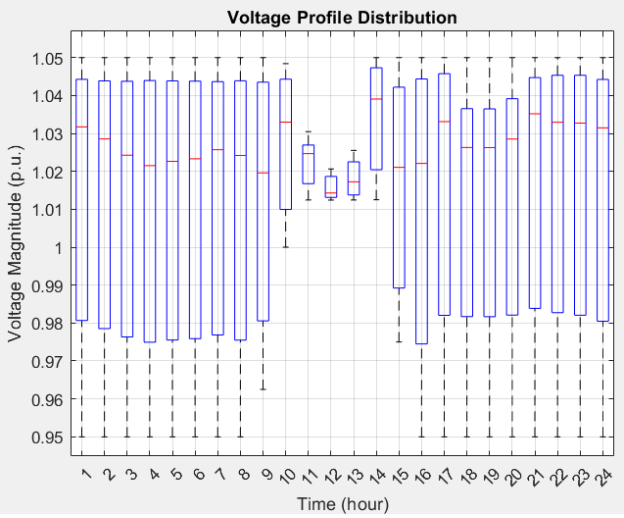

Figure 5: Voltage profile of case 3 (OLTC+CB+PV)

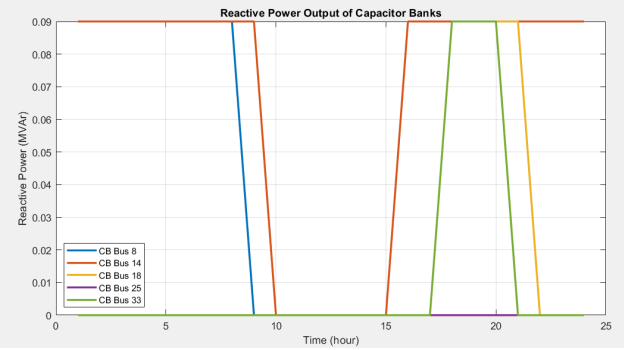

Figure 6: Reactive power of CBs of case 3 (OLTC+CB+PV)

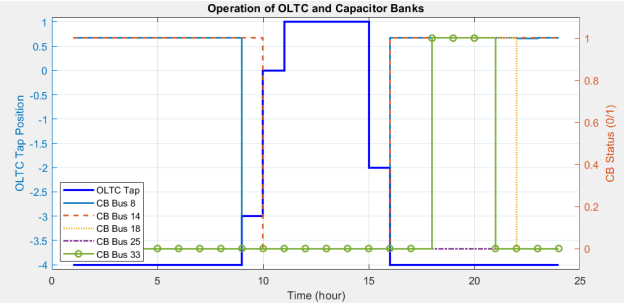

Figure 7: Operation of OLTC and CBs of case 3 (OLTC+CB+PV)

2 Part 2: Enhanced Volt/Var Control

2.1 Literature Review of Enhanced VVC

We review various existing works that enhances the conventional VVC beyond simple OLTC and CB coordination.

A robust MISOCP model is proposed in [2] for microgrid scheduling. It handles uncertainties while maintaining voltage and reactive power constraints, providing resilience oriented VVC in microgrids. The work in [3] optimizes the allocation of static VAR resources (capacitors) alongside PV-based distributed generation. It focuses on planning-based VVC through optimal allocation of reactive power compensation devices in radial networks. New optimization algorithms are proposed in [4] to specifically account for equipment opertaion loss. It considers the wear and efficiency impacts on voltage control devices (tap changers, capacitors), balancing voltage regulation effectiveness with equipment lifespan and operational costs. A coordinated control approach using network reconfiguration and Soft Open Points (SOPs) is proposed in [5] to simultaneously optimize both active and reactive power flow in distribution networks. An AI/ML approach is used in [6] leveraging constrained temporal convolutional networks. It employs deep learning with operational constraints and a corrective feedback loop to enable data-driven VVC that can adapt to changing grid conditions while maintaining reliability.

These approaches significantly improve upon conventional VVC by addressing key limitations such as uncertainty handling, equipment wear considerations, fast-responding power electronic devices, and intelligent adaptive control, extending the mechanical-only OLTC and CB paradigm to incorporate modern power electronic resources and advanced optimization techniques. We consider some of these contributions in our proposed multi-timescale framework: optimization techniques for handling PV uncertainty in Level 2 coordination, optimal resource allocation strategies for Level 3 planning, equipment degradation cost modeling in the objective function, integration of fast-responding power electronic devices (e.g., SVCs) in Level 1, and control algorithms that can enhance the coordination layer's decision-making capabilities across all timescales.

2.2 Limitation of OLTC and CB

The core limitations of a conventional model with only OLTC and CBs such as the base system for case 1 and 2 in part 1 are summarized below:

- **Timescale Coordination**: The model optimizes all devices together in a single time window without distinguishing different response capabilities.
- **Single Optimization Horizon**: The model uses the day-ahead optimization rather than a real-time control framework.
- **Lack of Fast-Response Mechanisms**: The model does not have explicit control strategy for rapid voltage fluctuations.
- **No Uncertainty Consideration**: The model does not account for PV uncertainty/variability.

2.3 Multi-Timescale Hierarchical Control

In order to address these limitations, with the main challenge being the coordination of real-time voltage control across different timescales, we propose a multi-timescale hierarchical control framework with three distinct levels, modified from [7].

- Level 1 provides local fast control on a seconds timescale, using PV inverters with volt-var droop control and Static Var Compensators (SVCs) for rapid voltage regulation.
  - Unlike traditional discrete control devices like CBs that provide fixed reactive power steps, SVCs offer more precise and continuous reactive power control within their operating range.
  - The SVC integration evaluates the synergistic benefits of combining discrete and continuous control strategies, in a network with high renewable penetration where rapid voltage variations require fast-responding compensation devices. The balance between CBs and SVCs provides insights into the trade-offs between control complexity and voltage regulation performance.
- Level 2 offers a coordination layer operating on a 5-minute timescale, coordinating reactive power resources across the network using voltage-based heuristic dispatch.
- Level 3 handles slow adjustment on an hourly basis, planning OLTC and CB operations based on forecasted conditions. This is the existing MISOCP model from part 1 with OLTC, CBs and PVs, with an improved objective function.

2.3.1 System model

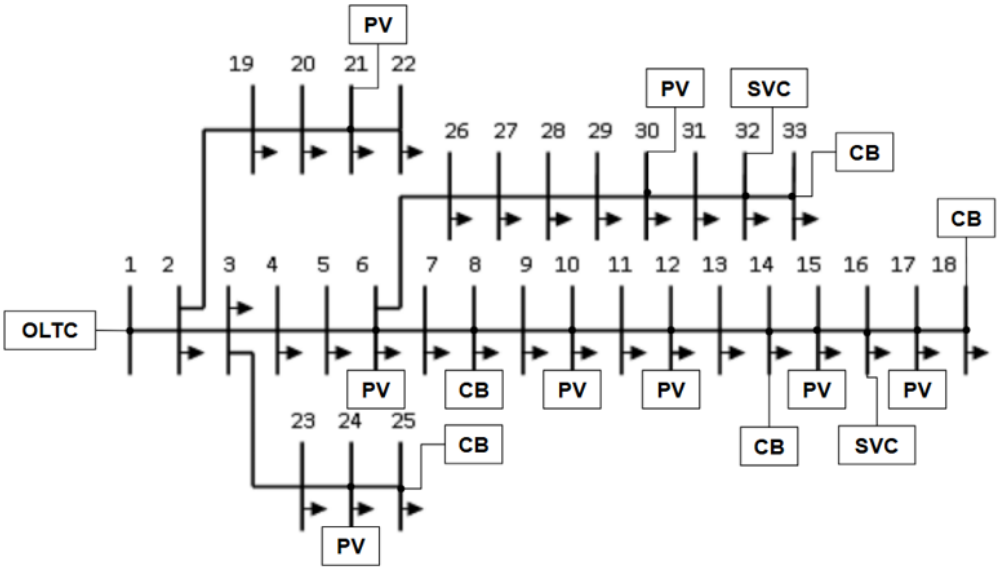

Figure 8: IEEE 33-bus system model of Multi-timescale case (OLTCs, CBs, PVs, and SVCs)

This enhanced IEEE 33-bus distribution system incorporates four voltage control devices operating under higher load conditions (1.0-2.0 p.u.): (1) an OLTC with ±12.5% regulation and 10 tap positions, (2) five 900 kVA CBs with 6-operation limits at buses 8, 14, 18, 25, and 33, (3) distributed PV generation totaling 600 kVA (46% penetration) at buses 6, 10, 12, 15, 17, 21, 24, and 30, and (4) two Static VAR Compensators (SVCs) rated at ±900 kVA each providing continuous reactive power control at buses 16 and 32.

This configuration represents a more complex voltage control scenario in which the addition of SVCs provides fast, continuous reactive power support to complement the discrete CB operations and OLTC tap changes, enabling effective voltage regulation under the increased loading conditions while managing the variability introduced by high PV penetration.

2.3.2 Parameters of Voltage Regulation Devices

Table 2: Parameters Of Voltage Regulation Devices

Device	Parameters	Operation Limits	Placement
OLTC	$\pm 12.5 \times 1\%$	10	1
CB1-5	900 kVar	6	8, 14, 18, 25, 33
PV1-8	600 kVA	-	6, 10, 12, 15, 17, 21, 24, 30
SVC1-2	$\pm$900 kVA	Continuous	16, 32

The enhanced multi-timescale VVC framework is implemented on the same IEEE 33-bus network with additional SVC devices for fast voltage regulation. The network parameters follow the standard IEEE 33-bus test system with capacity, operation parameters, and placement of voltage regulation devices as specified in Table 2. High-resolution PV variability scenarios are generated programmatically to simulate realistic solar intermittency including cloud variability, ramp rates, and minute-level fluctuations around the base hourly profiles.

The hierarchical control structure operates across three timescales. Fast local control (1-second resolution) for PV inverters and SVCs responding to voltage deviations through droop control. Coordination control (5-minute resolution) optimizing reactive power setpoints. Slow device scheduling (1-hour resolution) is for OLTC and CB operations. The framework demonstrates improved voltage regulation under rapid PV fluctuations compared to conventional single-timescale optimization approaches.

2.3.3 Mathematical Formulation

The proposed multi-timescale framework extends the conventional day-ahead centralized optimization by incorporating three distinct control layers operating at different timescales: 30 seconds for fast local control, minutes for coordination, and hours for slow device scheduling.

The enhanced MISOCP formulation minimizes network losses (19) subject to the constraints from conventional VVC including: power balance constraints (2) and coordination setpoint updates (16); line flow constraints with voltage drop constraints (3) and SOCP relaxation of power flow (4); voltage bounds and OLTC voltage constraints (5); OLTC tap change limits (6) with linearization (7); CB switching limits and reactive power injection (8) with linearization (9); and PV capability constraints (10) with piecewise linear approximation (11).

The framework introduces new constraint categories specific to multi-timescale coordination: fast local control droop responses for PV and SVC devices (12, 13) with reactive power limits (14); coordination layer heuristic dispatch (15, 16) with capability constraints (17) and voltage reference settings (18); cross-timescale coordination constraints (20, 21, 22, 23) that ensure coherent operation between different control layers; and time decomposition constraints (24) that define the temporal structure of the three-level hierarchy with 30-second, 5-minute, and 1-hour intervals respectively.

LEVEL 1: LOCAL FAST CONTROL (SECONDS)
These equations define the autonomous local control of PV inverters and SVC.

$$Q_{PV,i,t}^{fast} = Q_{PV,i}^{set} + K^{PV} \cdot (V_{ref,i} - \sqrt{v_{i,t-1}}) \quad \forall i \in N_{PV}, t \in T^{fast} \tag{12}$$

$$Q_{SVC,i,t}^{fast} = Q_{SVC,i}^{set} + K^{SVC} \cdot (V_{ref,i} - \sqrt{v_{i,t-1}}) \quad \forall i \in N_{SVC}, t \in T^{fast} \tag{13}$$

$$\Big\{ -Q_{max,i} \leq Q_{PV,i,t}^{fast} \leq Q_{max,i} \;\; -Q_{SVC,max} \leq Q_{SVC,i,t}^{fast} \leq Q_{SVC,max} \tag{14}$$

where $Q_{max,i} = \sqrt{\max(0, S_{rating,i}^2 - P_{PV,i,t}^2)}$ for PV capability limits.

LEVEL 2: COORDINATION LAYER (MINUTES)
This level uses voltage-based heuristic dispatch to update setpoints for fast-responding devices.

$$Q_{PV,i}^{set} = Q_{PV,i,t}^{current} + \alpha_{PV} \cdot (V_{target} - \sqrt{v_{i,t}}) \quad \forall i \in N_{PV} \tag{15}$$

$$Q_{SVC,j}^{set} = Q_{SVC,j,t}^{current} + \alpha_{SVC} \cdot (V_{target} - \sqrt{v_{j,t}}) \quad \forall j \in N_{SVC} \tag{16}$$

subject to:

$$\left\{-\sqrt{\max(0, S_{rating,i}^2 - P_{PV,i,t}^2)} \leq Q_{PV,i}^{set} \leq \sqrt{\max(0, S_{rating,i}^2 - P_{PV,i,t}^2)}\right. - Q_{SVC,max} \leq Q_{SVC,j}^{set} \leq Q_{SVC,max} \tag{17}$$

$$V_{ref,i} = V_{nom} \quad \forall i \in N_{PV} \cup N_{SVC} \tag{18}$$

LEVEL 3: SLOW DEVICE SCHEDULING (HOURS)
The slow device scheduling objective function minimizes network losses while penalizing frequent OLTC tap changes and CB switching operations. The MISOCP formulation is as follows.

$$\min J^{slow} = \sum_{t \in T^{slow}} \sum_{ij \in E} r_{ij} l_{ij,t} \tag{19}$$

Cross-timescale coordination is implemented through setpoint updates:

$$Q_{PV,i,t}^{fast} = f(Q_{PV,i}^{set}, V_{ref,i}, v_{i,t}) \quad \forall i \in N_{PV}, t \in T^{fast} \tag{20}$$

$$Q_{SVC,i,t}^{fast} = f(Q_{SVC,i}^{set}, V_{ref,i}, v_{i,t}) \quad \forall i \in N_{SVC}, t \in T^{fast} \tag{21}$$

$$Q_{CB,i,t} = \sum_{k} c_{ik,t} q_{ik} \quad \forall i \in N_{CB}, t \in T^{slow} \tag{22}$$

$$v_{1,t} = (V_s + tap_t \cdot \Delta V_T)^2 \quad \forall t \in T^{slow} \tag{23}$$

Time decomposition of the three-level hierarchy:

$$\begin{cases} T^{fast} & = t | t = k\Delta t^{fast}, k = 0, 1, 2, ..., \Delta t^{fast} = 30 \text{ seconds} \\ T^{coord} & = t | t = k\Delta t^{coord}, k = 0, 1, 2, ..., \Delta t^{coord} = 5 \text{ minutes} \\ T^{slow} & = t | t = k\Delta t^{slow}, k = 0, 1, 2, ..., \Delta t^{slow} = 1 \text{ hour} \end{cases} \tag{24}$$

2.3.4 Results

- Voltage regulation

Fig.9 shows the voltage profile distribution of the multi-timescale system. During early morning hours (1-8h), when both load demand and PV generation are minimal, the system exhibits tight voltage distributions centered around 0.96-0.97 p.u., with some buses approaching the minimum limit (0.95 p.u.). This indicates adequate voltage support during low-demand periods, though marginal violations suggest potential need for increased reactive power support.

During the peak operational period (midday hours [9-15h]), incurs peak PV generation. The voltage distributions show significant elevation, with median values reaching 1.02-1.04 p.u. and maximum voltages approaching the maximum limit (1.05 p.u.). The larger inter-quartile ranges during these hours indicate substantial voltage variations across the network, reflecting the localized impact of distributed PV generation and the system to maintain voltage regulation.

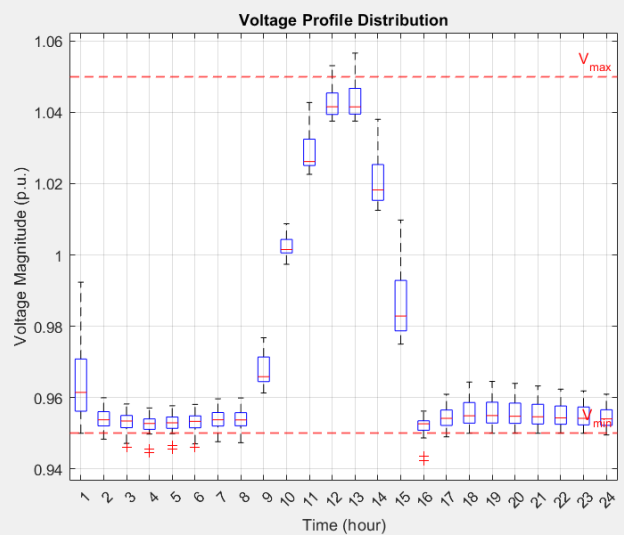

Figure 9: Voltage profile of multi-timescale system

- Reactive power coordination

The multi-timescale reactive power coordination in Fig.10 shows the hierarchical control strategy. The slow control layer (CBs) provides base reactive power support with step changes at hourly intervals, while fast control devices (PVs and SVCs) provide continuous fine-tuning.

During periods of high reactive power demand (hours 1-2 and 15-20), the system demonstrates coordinated response with CBs providing majority of the support and fast devices handling small adjustments. The negative reactive power injection by PV inverters during midday hours (10-14h) effectively counteracts over-voltage conditions caused by high PV active power generation. This behavior combined with OLTC tap adjustments demonstrates the system's ability to manage voltage rise in high-PV penetration networks.

- Multi-timescale control coordination

The control hierarchy in Fig.11 demonstrates coordination between slow and fast control layers. The OLTC operates as the primary slow control device, adjusting tap positions throughout the day. The tap progression shows proactive voltage regulation, with negative taps during low-voltage periods (early morning) and positive taps during high-voltage periods (midday PV generation). CB switching exhibits strategic deployment, with different CBs activated during distinct periods: CB Bus 8 operates during early morning, CB Bus 18 during mid-morning, and CBs Bus 25 and 33 during evening hours. This suggests the optimization algorithm is able to identify optimal locations and timing for reactive power injection based on network loading conditions.

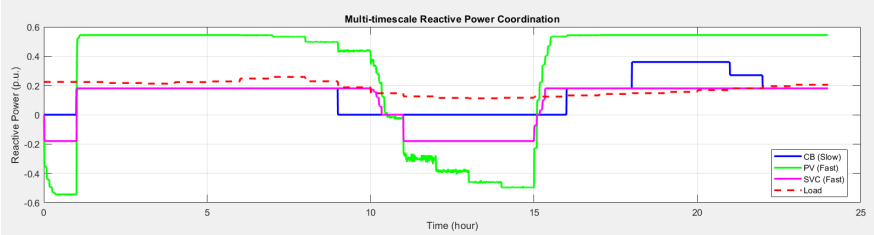

Figure 10: Reactive power coordination of multi-timescale system

The fast control layer (PVs and SVCs) provides continuous voltage support with response times of 30 seconds. PV reactive power control shows dynamic behavior, transitioning from capacitive operation (positive Q) during low-voltage periods to inductive operation (negative Q) during high-voltage periods. This demonstrates the PV inverters' capability to both support and absorb reactive power as needed for voltage regulation. SVCs exhibit rapid response with frequent adjustments between ± 0.09 p.u. limits. The coordination between PVs and SVCs shows complementary operation, where SVCs provide additional support when PV capability is insufficient, or when PV inverters are operating at their reactive power limits.

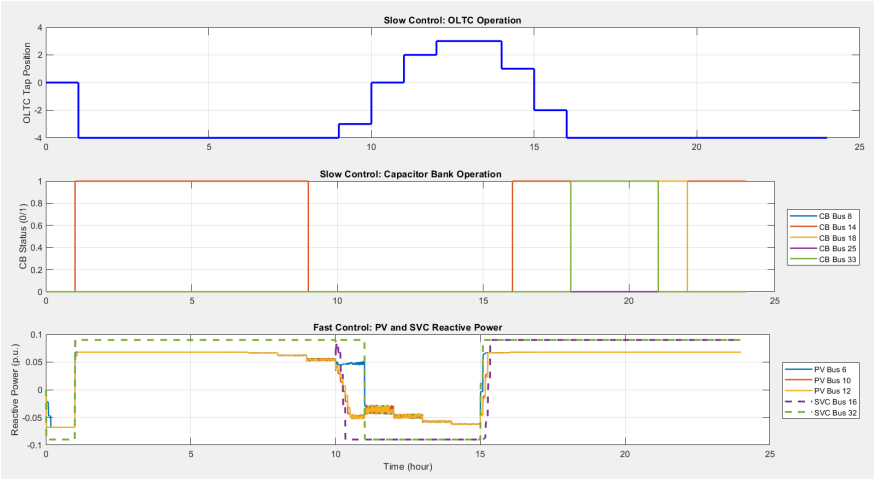

Figure 11: Operation of fast and slow control layer in multi-timescale system

3 MATLAB code

The code for Part 1 contains two MISOCP solvers, one for case 1 and 2 (OLTC+CB) and one for case 3 (OLTC+CB+PV). Note that the voltage bounds for case 1 and 2 are different and need to be set accordingly in the solver file. The optimization results are basecase_results_case1', 'basecase_results_case2' and 'optimization_results' for case 1, 2, 3, respectively. The PV and load profiles are generated from generated with 'generate_pv.m' and the CSV file, with samples already included in 'small load' and 'medium load' folders for demands of 0.2-0.5 p.u. and 0.5-1.0 p.u.. The 'vvc_plot.m' is used for generating the visuals included in this report.

The code for Part 2 contains a enhanced MISOCP solver and a 'enhanced_vvc_plot.m', using the medium-load PV and load profiles.

4 Video comments

"Work is of an outstanding quality that offers analysis and critical insight into the modelling and optimization context, data sources and cohort. Target issue(s) clearly defined and the scope of the problem

clear. Thoroughly considered rationale behind the selection of appropriate target issue(s) which is logically integrated with the context analysis.

Great job! Please provide some backgrounds for VVC (i.e., why VVC is needed, defining appropriate target issue)

(90/100)"

I have provided a "background" section in the final report to expand on the context for VVC implementation. I explained how VVC as a coordinated strategy is different from traditional reactive voltage control methods, and why it is needed by addressing challenges like bidirectional power flows, voltage rise, inadequate response speeds of conventional control devices etc.. Additionally, I identify the target issue: voltage violations across multiple operational timescales in modern distribution networks with high penetration. This is also the main issue tackled in Part 2 (Enhanced VVC) of this report.

References

[1] X. Sun and J. Qiu, "Two-stage volt/var control in active distribution networks with multi-agent deep reinforcement learning method," *IEEE Transactions on Smart Grid*, vol. 12, no. 4, pp. 2903–2912, 2021.

[2] N. M. Zografou-Barredo, C. Patsios, I. Sarantakos, P. Davison, S. L. Walker, and P. C. Taylor, "Microgrid resilience-oriented scheduling: A robust misocp model," *IEEE Transactions on Smart Grid*, vol. 12, no. 3, pp. 1867–1879, 2021.

[3] M. K. Islam, M. A. Habib, and M. J. Hossain, "Optimal allocation of pv based dg and capacitor in radial distribution network," *IEEE Access*, vol. 9, pp. 60 266–60 282, 2021.

[4] Y. Liu, Y. Gao, H. Yang, T. Li, and P. Ju, "The optimization for voltage and reactive power control of distribution network considering equipment operation loss," in *2021 IEEE 4th International Conference on Electronics and Communication Engineering (ICECE)*. IEEE, 2021, pp. 215–219.

[5] P. Li, W. Feng, J. Liu, G. Li, J. Dai, Z. Xie, and X. Ba, "Active and reactive power coordinated optimization of active distribution networks considering dynamic reconfiguration and sop," *IET Renewable Power Generation*, vol. 17, no. 11, pp. 2322–2334, 2023.

[6] Y. Chen, C. Li, C. Cao, J. Liu, H. Zhang, and Q. Wu, "Data-driven volt/var control based on constrained temporal convolutional networks with a corrective mechanism," *Electric Power Systems Research*, vol. 224, p. 109625, 2023.

[7] Y. Xu, Z. Y. Dong, R. Zhang, and D. J. Hill, "Multi-timescale coordinated voltage/var control of high renewable-penetrated distribution systems," *IEEE Transactions on Power Systems*, vol. 32, no. 6, pp. 4398–4408, 2017.